International Journal of Heat and Fluid Flow 30 (2009) 960–970

Contents lists available at ScienceDirect

International Journal of Heat and Fluid Flow

journal homepage: www.elsevier.com/locate/ijhff

Experimental and numerical analysis of spray-atomization characteristics of biodiesel fuel in various fuel and ambient temperatures conditions

Su Han Park, Hyung Jun Kim, Hyun Kyu Suh, Chang Sik Lee *

Graduate School of Hanyang University, Department of Mechanical Engineering, Hanyang University, 17 Haengdang-dong, Sungdong-gu, Seoul 133-791, Republic of Korea

ARTICLE INFO

Article history:
Received 22 November 2008
Received in revised form 4 February 2009
Accepted 9 April 2009
Available online 19 May 2009

Keywords:
Fuel temperature
Evaporation
Sauter mean diameter (SMD)
Soybean oil methyl ester (SME)
Spray axial distance

ABSTRACT

The purpose of this work is to reveal the effects of fuel temperatures and ambient gas conditions on the spray-atomization behavior of soybean oil methyl ester (SME) fuel. The spray-atomization behavior was analyzed through spray parameters such as the axial distance from the nozzle tip, local and overall Sauter mean diameter (SMD). These parameters were obtained from a spray visualization system and a droplet measuring system. In addition, the experimental results were compared with the numerical results calculated by the KIVA-3V code. It was revealed that the increase of the fuel temperature (from 300 K to 360 K) little affects the spray liquid tip penetration. The increase of the ambient gas temperature (from 300 K to 450 K) caused a increase in the spray liquid tip penetration. Also, biodiesel fuel evaporation actively occurred due to the increase in the fuel temperature and the ambient gas temperature. Of special significance was that the highest vapor fuel mass concentration was observed at the center region of the spray axis. In the results of the microscopic characteristics, the detected local droplet size at the axial direction and overall droplet size at the axial and radial direction in a control volume increased when the fuel temperature increased. This is believed to be due to an increase in the number of small droplets that quickly evaporated. In addition, the increased fuel temperature caused the decrease of the number of droplets and the increase of the vapor fuel mass. The mean axial velocity of droplets decreased with increasing fuel temperature.

1. Introduction

Combustion and emission performance of a diesel engine are governed by the mixture quality of the injected fuel and the intake air. A homogeneous mixture reduces the emission of particulate matter (PM), as well as improves the combustion efficiency of an engine. The air-fuel mixture in the combustion chamber is affected by the fuel properties, such as fuel density, viscosity, and surface tension, and mixing rate between fuel and intake air. The variation of fuel properties according to the temperature were studied by Yoon et al. (2008). They found that fuel density decreases linearly and the kinematic viscosity decreases exponentially with increasing fuel temperature. Presently, studies related with these facts about the spray characteristics based on the variation of fuel temperature are progressing.

Kawano et al. (2004) studied about the flash boiling characteristics of multi-component fuel, and investigated the effect of the initial fuel temperature on the flash boiling, experimentally and numerically. They reported that the increase of the initial fuel temperature induced the decrease of the spray tip penetration, because of the evaporation of fuel with low boiling point. In addition, they confirmed that the flash boiling effectively accelerated the atomization and vaporization of fuel droplets.

Biodiesel is a renewable, oxygenated fuel that has a high cetane number. It is considered to be a next generation, environmental friendly alternative fuel to conventional diesel fuel. In light of these things, studies related with biodiesel fuel are progressing actively, nowadays (Kegl et al., 2006; Suh et al., 2008; Ahmed et al., 2006). Biodiesel fuel has a higher viscosity, specific gravity, density, and cloud point than does an ultra low sulfur diesel (ULSD). These features have a significant influence on fuel spray, atomization, and evaporation characteristics. The study on the spray characteristics of alternative fuel in the engine is essential, because the combustion and emissions performance of a diesel engine was greatly influenced by the overall spray characteristics and fuel properties.

In this work, macroscopic spray characteristics including spray tip penetration were analyzed by using spray images obtained from the visualization system, as illustrated in Fig. 1. Spray tip penetration is defined as the maximum distance from a nozzle tip that an injected spray can reach. Studies about spray tip penetration are currently ongoing, and empirical and theoretical equations were suggested by many researchers (Hiroyasu and Arai, 1990; Desantes et al., 2006). In their research, spray tip penetration was affected by the relative magnitude of two opposing forces: the kinetic energy of the initial liquid jet and the aerodynamic resistance of the

* Corresponding author. Tel.: +82 2 2220 0427; fax: +82 2 2281 5286.
E-mail address: cslee@hanyang.ac.kr (C.S. Lee).

0142-727X/$ - see front matter © 2009 Elsevier Inc. All rights reserved.
doi:10.1016/j.ijheatfluidflow.2009.04.003

Nomenclature

A_{hole}	hole area
A_{vena}	vena contracta area
B	mass transfer rate
C_C	ratio of concentration area and nozzle area
C_d	discharge coefficient
D_{eff}	cross-sectional of the initial blob
K_{inlet}	inlet loss coefficient
L_R	radial distance from the spray axis
L_Z	axial distance from the nozzle tip
L/D	orifice length/hole diameter
$m_{injected}$	injected mass flow
Nu	Nusslet number
P_{amb}	ambient pressure
P_{inj}	injection pressure
P_{vapor}	vapor pressure
P_1, P_2	inlet and outlet pressure
Pr	Prandtl number
R/D	orifice inlet radius/hole diameter
Re	Reynolds number
S_C	Schmidt number
Sh	Sherwood number
T_{amb}	ambient gas temperature
T_{fuel}	fuel temperature
t_{asoi}	time after start of injection
t_D	detecting time
t_{eng}	energizing duration
U_{eff}	effective injection velocity
U_{mean}	mean velocity
U_{vena}	flow velocity in the vena contracta
Y_∞	mass fraction of fuel vapor (free stream condition)
Y_S	mass fraction of fuel vapor (droplet surface)
ρ_{liquid}	liquid density

surrounding gas. An over penetration of spray is one reason for fuel impingement on the combustion chamber walls. An inadequate penetration of spray causes an unsatisfactory fuel–air mixture. For these reasons, an optimal engine performance is obtained when the spray tip penetration is matched to the size and geometry of the combustion chamber (Lefebvre, 1989).

In spite of the importance of fuel temperature on the macroscopic and microscopic spray characteristics (Kim et al., 2007), there are uncertainties regarding the atomization and vaporization characteristics of biodiesel fuel spray in the combustion chamber. As a result, this study investigated the effect of fuel temperature on the spray, atomization and evaporation characteristics of biodiesel fuel, both experimentally and numerically, for improved investigation. Unlike previous research (Kawano et al., 2004), the experimental device used in this work minimizes the thermal loss of test fuel in a fuel supply line, and improves experimental accuracy by heating the fuel supply line with the duplication tube. In order to study the spray characteristics, the spray shape, and spray tip penetration were investigated. The spray shape images obtained from the experiment were compared to the calculated spray images, and the experimental results of the spay tip penetration were compared to the calculated results. The injection quantity and injection rate profile were measured experimentally, and applied for the calculation in KIVA-3V code. At the same time, the local and overall Sauter mean diameter (SMD) and detected droplet distribution were also investigated to analyze atomization characteristics under various fuel temperatures. Finally, spray evaporation characteristics with respect to variation in fuel temperature were numerically analyzed.

2. Experimental setup and procedure

2.1. Experimental setup

Two test injectors were used to investigate the atomization and spray characteristics of biodiesel fuel, as shown in Fig. 2. A single hole nozzle injector with a 0.3 mm diameter and a 0.8 mm orifice depth ($L/D = 2.67$) was used to analyze atomization performance. In addition, a six-hole nozzle injector with 0.126 mm orifice diameters and a 156° spray angle was utilized for studying the macroscopic spray characteristics.

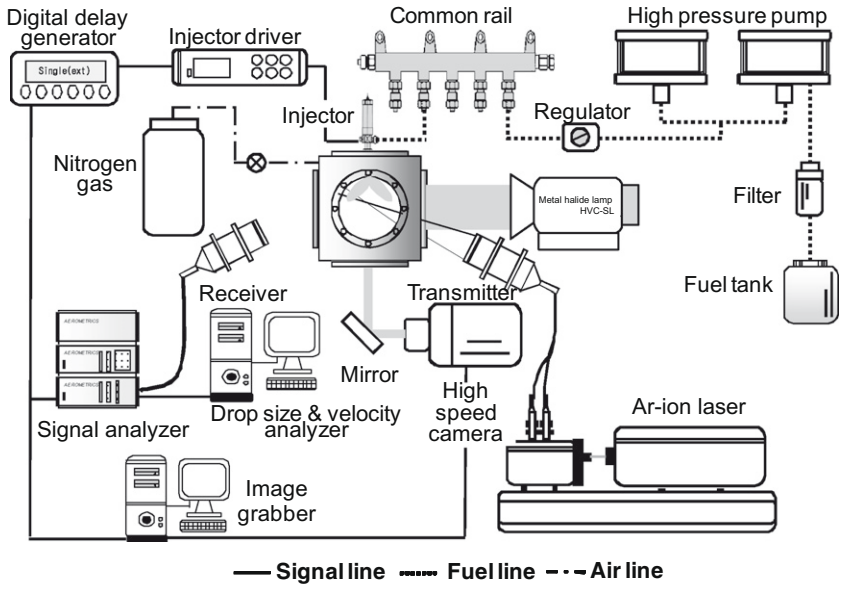

Fig. 1. Schematic of droplet measuring system and visualization system.

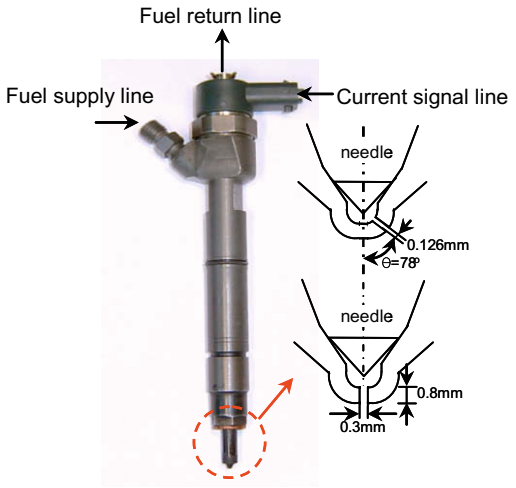

Fig. 2. Test injectors with single and six-holes nozzle.

In order to obtain spray images at the various injection conditions, a visualization and droplet measuring system were installed as shown in Fig. 1. Spray images of a bottom view type were obtained by using a high speed camera (Photron, Fastcam-APX RS) with two metal-halide lamps (Photron, HVC-SL) as the light source. To synchronize the fuel injection and camera shutter signal, a multi-channel digital delay/pulse generator (Berkeley Nucleonics Corp., Model 555) and an image grabber installed in a computer were installed, and the operation of the test injector was controlled by an injector driver (TEMS, TDA-3200H).

It is already reported by many researchers (Araneo et al., 2006; Lacoste et al., 2003) that to measure the dense biodiesel spray is very difficult. Therefore, the droplet measuring system was optimized with reference to papers of Araneo et al. (2006) and Lacoste et al. (2003). The droplet measuring system consisted of an Ar-ion laser (INNOVA 70C, Coherent) with 2.0 W laser output, and PMT (photomultiplier tube) voltage of 500 V, a transmitter, a receiver, and a droplet size and velocity analyzer. In order to obtain time resolved data, the signal analyzer was synchronized with the injector driver by using a digital delay/pulse generator.

Fig. 3 shows the fuel heating device and a high pressure chamber. Biodiesel fuel was heated by high pressure and high temperature steam generated from a boiler. While the biodiesel fuel went through the fuel supply line wrapped by a duplication tube, the fuel temperature of biodiesel was varied to 300 K, 330 K and 360 K, successively. Fuel temperature and steam temperature were measured by two *K*-type thermocouples (Omega, KMTSS-020G-12), one in the fuel supply line, and the other in the duplication tube. Fuel temperature was controlled by the relief valve. In addition, the high pressure chamber was heated by a heating coil in order to investigate the effect of the ambient gas temperature on the spray development process. In addition, the ambient gas in a high pressure chamber pressurized by the nitrogen gas to 4 MPa (maximum).

Table 1
Specification of the droplet measuring system.

Light source	Ar-ion laser
Wave length	514.5 nm, 488 nm
Focal length	500 mm for transmitter and receiver
Collection angle	30°

2.2. Experimental procedure

In order to study the effect of fuel temperature and ambient gas temperatures on the spray characteristics of biodiesel fuel, the fuel and ambient gas temperature were adjusted from 300 K to 360 K and from 300 K to 450 K, respectively.

For investigating atomization performance, the diameter subrange for the droplet measurement was set from 1.5 μm to 75 μm, and approximately 5000 spray droplets were averaged at each measuring point. The measuring points were located every 2 mm and 5 mm in the radial and axial distance from the nozzle exit, respectively. The measurement program terminated when the droplet measuring system obtained 5000 spray droplets, and this process was repeated two times. In this case, the measuring time of droplets is called the detecting time (t_D). The detailed specification and criteria for the droplet measuring system, and the setup of high speed camera for the visualization system are listed in Tables 1 and 2. The experimental conditions are explained in Table 3.

In this work, biodiesel fuel was derived from soybean oil (soybean oil methyl ester or SME) and was used for investigating the spray-atomization characteristics of fuel at various temperatures. The specifications of biodiesel fuel used in this study are listed in Table 4. In general, combustion–emission characteristics are closely connected to the spray-atomization characteristics; therefore, the information about the fuel properties is very important in order to grasp these characteristics.

Fig. 4 shows the characteristics of fuel properties of biodiesel fuel according to the variation of the fuel temperature (Park et al., 2008). As confirmed in Fig. 4, with increasing fuel temperature, fuel density decreases linearly and kinematic viscosity decreases exponentially.

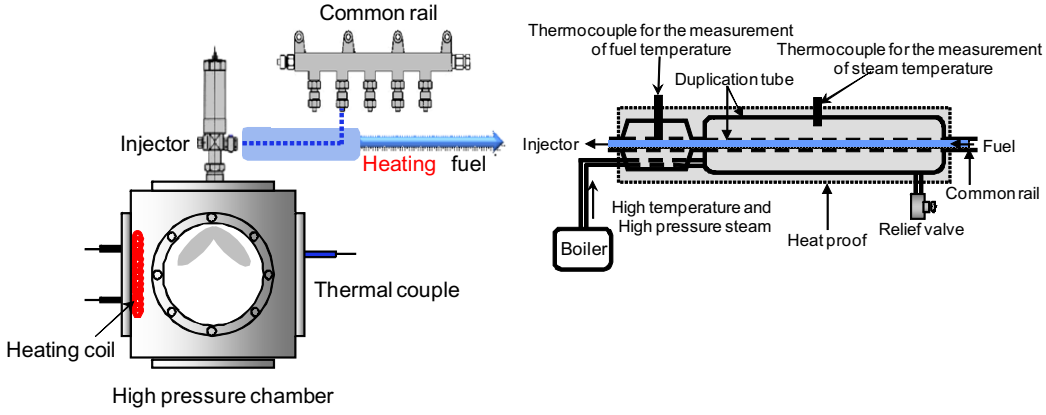

Fig. 3. Fuel heating system and high pressure chamber.

Table 2
Criteria for droplet measurement and set-up of high speed camera.

Criteria for droplet measurement	
Burst threshold (mV)	0.5
Mixer frequency (MHz)	36
Filter frequency (MHz)	40
PMT voltage (V)	500
Signal-to-noise ratio	65
Diameter sub-range (μm)	1.5–75
Set-up of high speed camera	
Frame rate (fps)	10000
Shutter speed (s)	1/20000
Resolution	512 × 512

Table 3
Experimental conditions for spray visualization and droplet measurement.

Spray visualization	Injection pressure (P_{inj}, MPa)	60, 120
	Ambient pressure (P_{amb}, MPa)	2.0, 4.0
	Energizing duration (t_{eng}, ms)	1.0
	Fuel temperature (T_{fuel}, K)	300, 330, 360
	Ambient temperature (T_{amb}, K)	300, 400, 450
Droplet measurement	Injection pressure (P_{inj}, MPa)	60
	Ambient pressure (P_{amb}, MPa)	0.1
	Energizing duration (t_{eng}, ms)	0.5
	Fuel temperature (T_{fuel}, K)	300, 330, 360
	Ambient temperature (T_{amb}, K)	300

Table 4
Specifications of test fuels[a].

Fuel property	Biodiesel
Fuel standard	ASTM D 6751
Lower heating value, Btu/gal	~118,170
Kinematic viscosity, *cP* @ 40 °C	4.0–6.0
Specific gravity, kg/l @ 16 °C	0.88
Density, lb/gal @ 15 °C	7.328
Water and sediment, vol%	0.05max
Carbon, wt%	77
Hydrogen, wt%	12
Oxygen, by dif. Wt%	11
Sulfur, wt%	0.0024–0.01
Boiling point, °C	315–350
Flash point, °C	100–170
Cloud point, °C	−3 to 12
Pour point, °C	−15 to 10
Cetane Number	48–65
Lubricity SLBOCLE, grams	>7000
Lubricity HFRR, microns	<300

[a] Biodiesel handling and use guidelines Energy Efficiency and Renewable Energy DOE/GO-102006-2358 third edition September 2006.

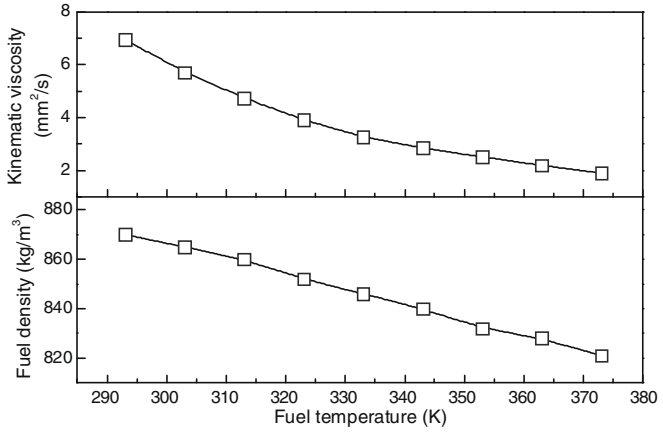

Fig. 4. Characteristics of fuel properties of biodiesel according to the variation of fuel temperature (Park et al., 2008).

3. Numerical methods

3.1. Applied biodiesel fuel in the KIVA code

In order to apply the biodiesel fuel in the KIVA code, the spray characteristics of biodiesel fuel were calculated by an insertion of their fuel properties into the KIVA fuel library. Yoon et al. (2008) conducted the experimental investigation of the fuel properties of diesel and biodiesel fuels, such as a fuel density, kinematic and dynamic viscosity for the variation of the fuel temperature. They measured the specific gravity and dynamic viscosity of test fuels by using a hydrometer and a viscometer, respectively. From these measurements, the fuel library of biodiesel fuel spray was inserted into the KIVA code, and the atomization characteristics of fuels were calculated. The two-dimensional computational grid with 100 mm in width and 500 mm in length, and three-dimensional cylindrical grid with 120 mm in radius and 50 mm in height were used for the numerical analysis on the atomization of single hole injector and spray behaviors of six-holes injector as illustrated in Fig. 5a. Numbers of cells in the two-dimensional and three-dimensional computation grid are about 39,000 and 25,000 cells, respectively. In addition, the initial time interval set up the 20 μs, and the injection rate and fuel quantity at the experimental conditions put in the initial injection parameters of KIVA-3V code as shown in Fig. 5b.

3.2. Nozzle flow model

When the fuel was injected, a cavitation region appeared inside the nozzle orifice. This was due to a drop in the flow pressure of the fuel caused by an increase in the flow velocity. The initial blob size and velocity at the nozzle exit were greatly influenced by the cavitation region. This cavitation phenomenon plays an important role in droplet atomization after the start of injection. The internal flow in the nozzle orifice can be analyzed based on the assumption that the input parameters, such as the injected mass flow rate, the geometric diameter, the ambient pressure, the inlet radius/hole diameter (R/D) ratio and the nozzle orifice depth/hole diameter (L/D) ratio, are known (Sarre et al., 1999; Zhu et al., 2000; Bianchi et al., 2003; Ning et al., 2008).

As can be seen in Fig. 6, the inlet pressure at point 1 (p_1) can be estimated by using the Bernoulli equation presupposing turbulent flow, as given by following equation

$$p_1 = p_2 + \frac{\rho_{liquid}}{2}\left(\frac{U_{mean}}{C_d}\right)^2 \tag{1}$$

where $U_{mean} = m_{injected}/(A_{hole}\rho_{liquid})$ is the mean velocity of inner nozzle hole. The discharge coefficient (C_d) related to the inlet loss coefficient (K_{inlet}) and the wall friction loss is calculated as (Benedict, 1980)

$$C_d = (K_{inlet} + f \cdot (L/D) + 1)^{-0.5} \tag{2}$$

where $f = \max(0.316\mathrm{Re}^{-0.25}, 64/\mathrm{Re})$, and the inlet loss coefficient (K_{inlet}) is obtained from a tabulated value according to the R/D ratio.

The contraction of the flow area at the vena contracta, and the velocity at the smallest flow area were calculated using Nurick's expression and mass conservation as given by Nurick (1976)

$$A_{vena} = A_{hole}C_c, \quad U_{vena} = \frac{\dot{m}_{injected}}{A_{hole}C_c\rho_{liquid}} = \frac{U_{mean}}{C_c} \tag{3}$$

$$C_c = \left[(1/0.61)^2 - 11.4(R/D)\right]^{-0.5} \tag{4}$$

When the pressure at the vena contracta was lower than the vapor pressure (p_{vapor}), the flow in the nozzle was in full cavitation. In this case, the new inlet pressure (P_1) and discharge coefficient (C_d) were calculated using the following equations:

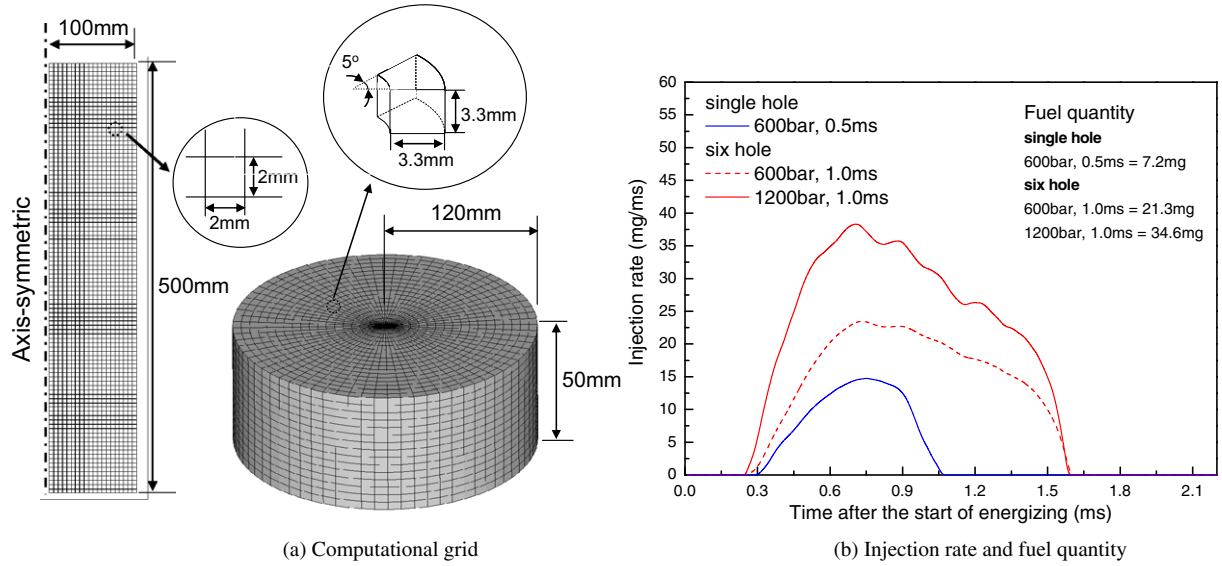

(a) Computational grid (b) Injection rate and fuel quantity

Fig. 5. (a) Computational grid for the numerical analysis and (b) injection rate and fuel quantity according to the experimental conditions.

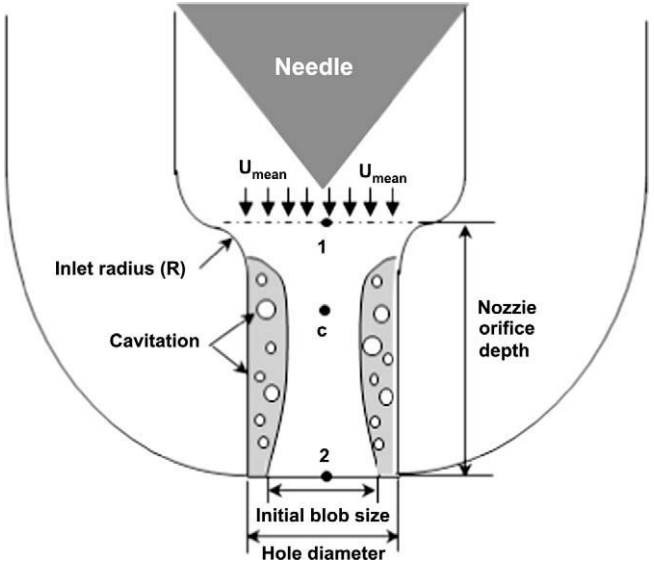

Fig. 6. Schematic of the cavitating nozzle.

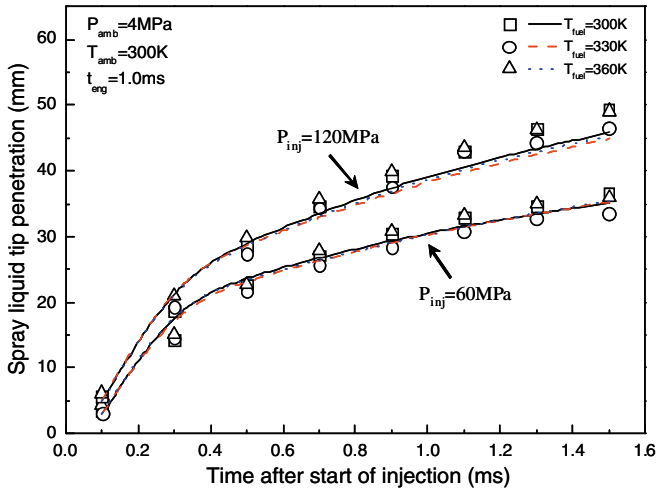

Fig. 7. Effect of the fuel temperature on the spray tip penetration of biodiesel fuel (symbols – measured results, lines – calculated results, P_{amb} = 4.0 MPa, t_{eng}=1.0 ms).

$$P_1 = p_{vapor} + \frac{\rho_{liquid}}{2} U_{vena}^2, \quad C_d = C_c \sqrt{\frac{p_1 - p_{vapor}}{p_1 - p_2}} \tag{5}$$

In the case of turbulent flow in the nozzle exit, the initial droplet size was equal to the nozzle hole diameter and the injection velocity at the exit was calculated using the volumetric mean velocity. In case of the super cavitation in the nozzle flow, the cross-sectional area of the initial blob (D_{eff}) is more diminished in size than the diameter of nozzle exit. In addition, the injection velocity (U_{eff}) increased by the application of momentum equilibrium from the point c to 2 as follows

$$U_{eff} = U_{vena} - \frac{p_2 - p_{vapor}}{\rho_{liquid} \cdot U_{mean}} \tag{6}$$

3.3. Atomization model

In order to set up the initial condition in the atomization model, the predicted initial droplet diameter and velocity in the nozzle exit were applied to calculate the breakup of the fuel spray. A hybrid breakup model was combined with the primary and secondary breakup models to analyze the fuel atomization characteristics in a common-rail injection system.

The WAVE breakup model (Reitz, 1987) is based on the growth of KH instabilities on the liquid surface at the interface between the injected fuel spray and ambient gas, which have different densities. This model is used for the primary breakup process in the hybrid model. In addition, the secondary breakup process was calculated using the RT breakup mechanism (Bellman and Pennington, 1954) which reflected the atomization characteristics by the RT instabilities. The RT instability resulted from the effect of deceleration of the droplets in the breakup process. The constants in the WAVE-RT hybrid breakup model were modified after comparing experimental results, such as the as the axial, radial distance and SMD value. The size and time constant in the WAVE breakup model were adjusted to be 0.61 and 100, respectively, in the present study. In addition, the breakup constants which related to the droplet size and time in the RT model were chosen as 0.1 and 1.0, respectively.

3.4. Evaporation model

The evaporation characteristics of the fuels were investigated with the droplet numbers and vaporized fuel mass calculated by using the basic evaporation model based on the lumped body theory (Amsden et al., 1989). Presupposing quasi-steadiness in the gas flow and even temperature droplets, heat and mass transfer occurred between a flowing fluid and a spherical droplet. The Nusslet and Sherwood numbers are expressed by the Ranz and Marshall correlation (Ranz and Marshall, 1952)

$$\mathrm{Nu} = 2 + 0.6\sqrt{\mathrm{Re}}\mathrm{Pr}^{0.33} \tag{7}$$

$$\mathrm{Sh} = 2 + 0.6\sqrt{\mathrm{Re}}\mathrm{Sc}^{0.33} \tag{8}$$

The mass transfer rate ($\dot{m}$) from a droplet in a steady state is calculated by using a correlation suggested by the Frossling (Faeth, 1977)

$$\dot{m} = 2\pi r(\rho D)_{air} B \times \mathrm{Sh} \tag{9}$$

where $(\rho D)_{air}$ is fuel vapor diffusivity in the air, and the mass transfer number (B) is given by following equation

$$B = \frac{Y_s - Y_\infty}{1 - Y_s} \tag{10}$$

In the above equation, Y is the mass fraction of the fuel vapor, and the subscript ∞ and s indicate the free stream condition and the droplet surface, respectively.

4. Results and discussion

4.1. Spray and evaporation characteristics of biodiesel fuel

Fig. 7 shows the characteristics of the spray tip penetration for injection pressures and fuel temperatures. Symbols and lines mean experimental and numerical results, respectively. As represented in Fig. 7, the spray tip penetration increased with the increase of the injection pressure. The increasing injection pressure caused an increase of the initial spray momentum. Spray tip penetration was only slightly affected by the variation in the fuel temperature, as shown in the experimental and numerical analysis. Therefore, it can be said that the spray tip penetration was not remarkably affected by a change in the fuel properties caused by the variation of fuel temperature. The numerical results agreed well with experimental results, in general. However, the numerical results were underestimated compared to the experimental results at 120 MPa of injection pressure from 0.7 ms after the start of the

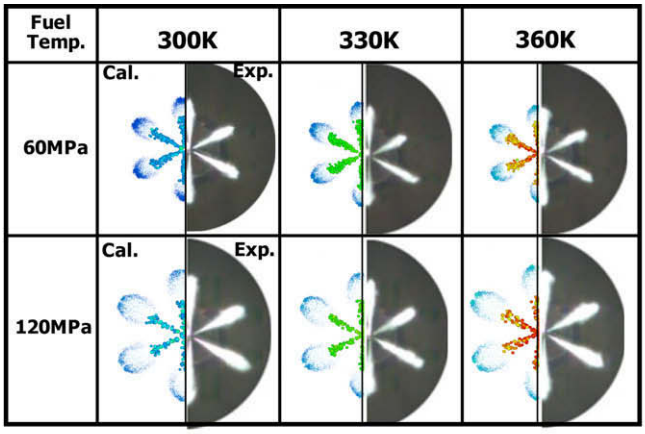

(a) t_{asoi} = 0.6 ms

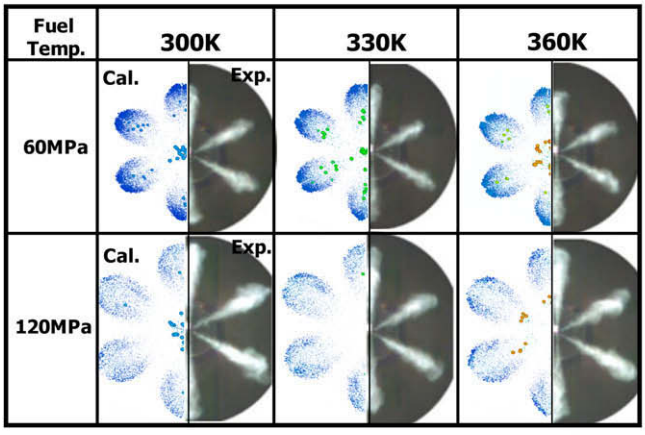

(b) t_{asoi} = 1.2 ms

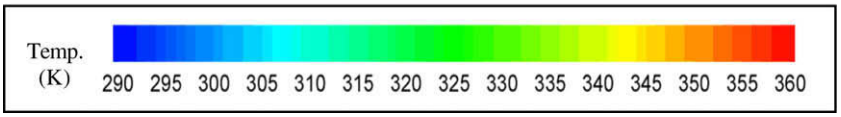

Fig. 8. Comparison of the spray images between experimental and numerical results at various injection pressures and fuel temperatures (P_{amb} = 4.0 MPa, t_{eng} = 1.0 ms).

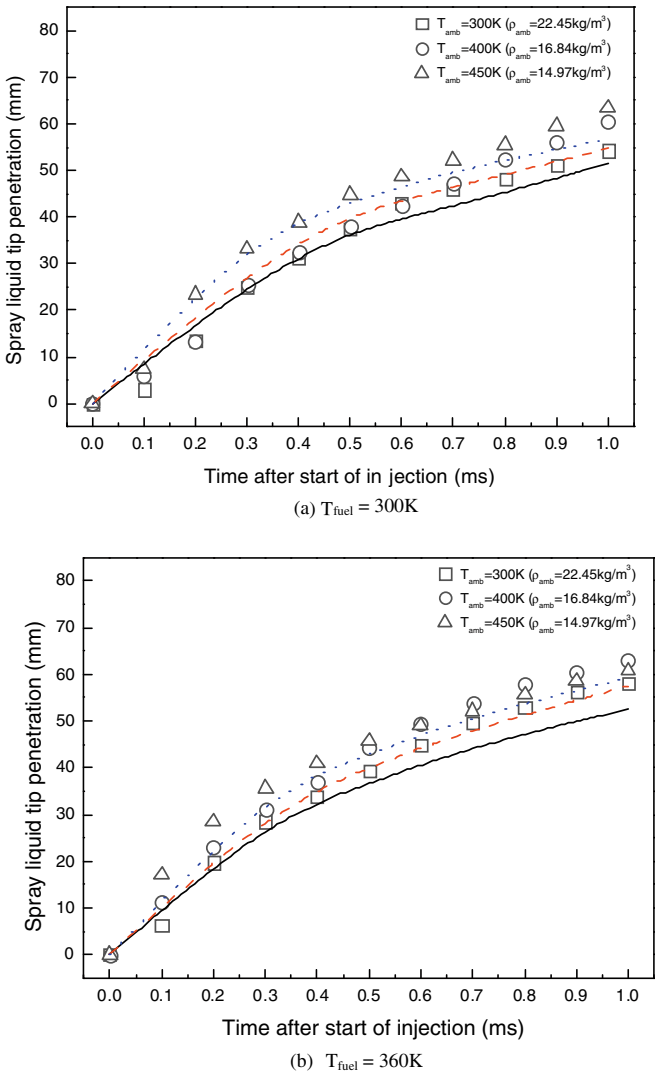

Fig. 9. Spray axial distance from the nozzle tip and tip velocity of biodiesel fuel on the variation of ambient gas temperature at two fuel temperature conditions (symbols – experimental results, lines – numerical results, P_{inj} = 120 MPa, P_{amb} = 2 MPa, t_{eng} = 1.0 ms).

injection. It is postulated that excessive breakups in a downstream of the spray were predicted by the secondary breakup model.

Comparisons of the spray images between experimental and numerical results at the same injection and ambient conditions (i.e., injection pressure, ambient pressure, fuel temperature, and time after start of injection) are illustrated in Fig. 8. Fig. 8a and b shows results at 0.6 ms and 1.2 ms of time after the start of injection. The color variation in the numerical results indicates change in fuel temperature distribution. The numerical results in Fig. 8 show a detailed vortex and mixing between the injected spray droplets and the ambient gas which were not represent in the experimental results. Fig. 8 also shows an excellent correlation between images thus demonstrating that not only the spray axial distance, but also the spray structure and shape are correctly predicted by the KIVA-3V code. Especially, as the time after the start of injection elapsed, the numerical results illustrated active fuel evaporation and atomization performance by the reduction of the droplet number and droplet size.

Fig. 9 shows the effect of ambient temperature on the spray tip penetration of biodiesel fuel under the 120 MPa of injection pressure, 2 MPa of ambient gas pressure, and 1.0 ms of energizing duration. As illustrated in Fig. 9a and b, the increased ambient air temperature induced the increase of the spray liquid tip penetration, because the ambient air density decreased with the increase of the ambient air temperature. In Fig. 9, the numerical results consistently underestimated the experimental results. The secondary breakup processes are actively progressing due to the reduction of fuel surface tension and density which are the main parameters determining the droplet size, after the growth of waves in the KH model. In addition, the evaporation model somewhat affected the reduction of the spray tip penetration.

Fig. 10 also shows the comparison between the experimental and calculated spray images under the various injection conditions at t_{asoi} = 1.0 ms. The color legend in the calculated results means the distribution of the fuel temperature. As illustrated in Fig. 10, it can be confirmed that the temperature of the injected spray was affected by the ambient gas temperature. Therefore, the properties of the injected spray were changed by the ambient gas temperature and the fuel temperature. Based on these results, the increase of the ambient gas temperature and the fuel temperature caused the reduction of the fuel droplet distribution and the number of droplets by the fuel evaporation. On the other hand, it seemed that the spray cone angle of the calculated spray is larger

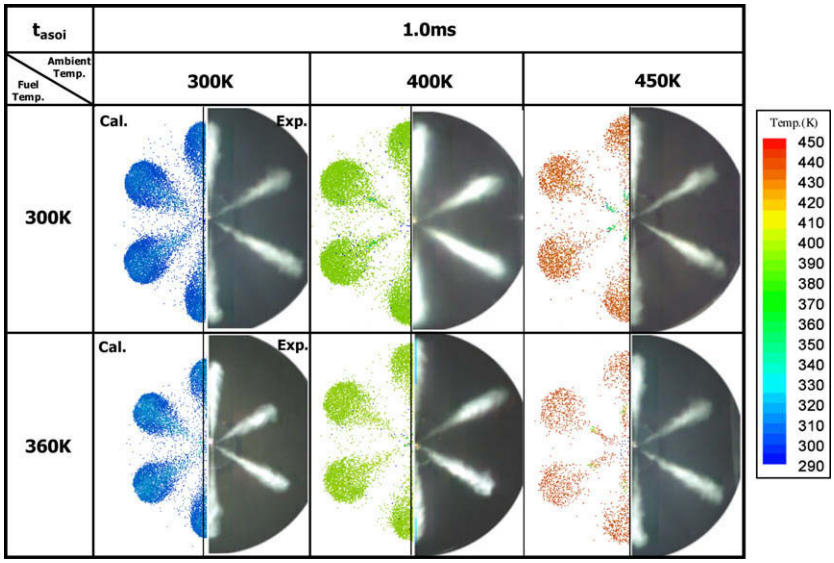

Fig. 10. Comparison of the experimental and calculated spray images under the various injection conditions at t_{asoi} = 1.0 ms (P_{inj} = 120 MPa, P_{amb} = 2.0 MPa, t_{eng} = 1.0 ms).

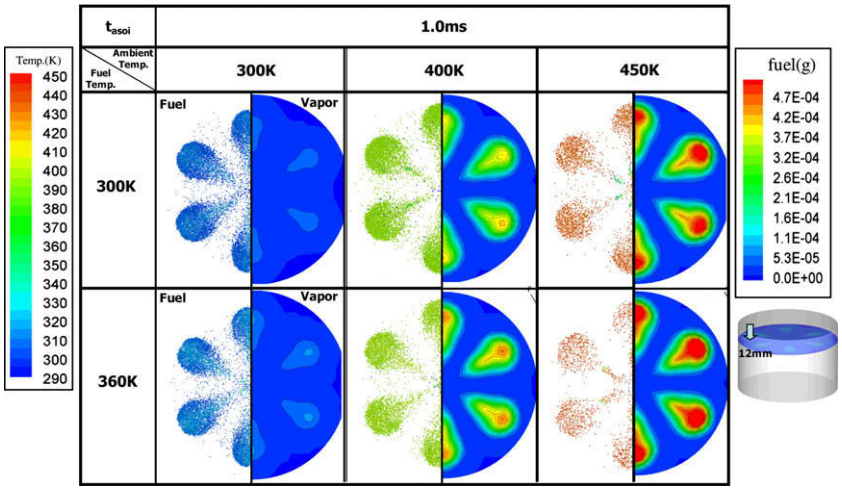

Fig. 11. Spray and evaporation characteristics under the various ambient and fuel temperature at time after start of injection 1.0 ms (P_{inj} = 120 MPa, P_{amb} = 2.0 MPa, t_{eng} = 1.0 ms).

than that of the experimental spray. It is guessed that the vortex phenomena under the high ambient pressure were overestimated in the calculation results. The numerical results predicted well the experimental results.

The calculated spray and evaporation characteristics under the various ambient gas temperatures and fuel temperatures at the time after start of injection 1.0 ms are shown in Fig. 11. The left side of Fig. 11 shows the injected fuel droplet distributions and their temperature distribution, while the right side shows the vapor mass distribution. As shown in the right images of Fig. 11, the most fuel evaporation actively occurs at the center of the spray, and the evaporation mass is the highest at the spray axis, because the droplets of injected spray are aggregated at the center of the spray. In addition, the evaporated fuel mass certainly increased as the ambient air temperature increased to 450 K. Hence, it can be confirmed that the fuel evaporation mass was mainly affected by the ambient air temperature. From these results, it can be expected that the active fuel evaporation by the increase of the fuel and ambient air temperature influences the formation of the homogeneous mixture between the injected fuel spray and ambient air.

4.2. Atomization performance of biodiesel fuel at various fuel temperature conditions

In most combustion systems, fuel atomization performance leads to a wider combustion range and low pollutant exhaust emissions. Therefore, a study of fuel atomization should be conducted to optimize combustion systems. Thus, atomization performance of biodiesel fuel in different fuel temperature conditions was investigated. The results were compared in terms of the detected local SMD and the detected droplet percentage by using a droplet measuring system. At the same time, obtained experimental results were compared with numerical results by using the KIVA-3V code.

Fig. 12 shows the effect of fuel temperature on the local and overall SMD characteristics of biodiesel fuel. As represented in Fig. 12a, the detected local SMD increased when the fuel temperature increased both experimentally and numerically. However, these results do not mean that the size of each droplet size increased. These results caused by the decrease of the small droplets in the detecting volume and the remains of the large droplets. Instead, these results suggest that the small droplets in the detecting volume are more easily evaporated, while the large droplets re-

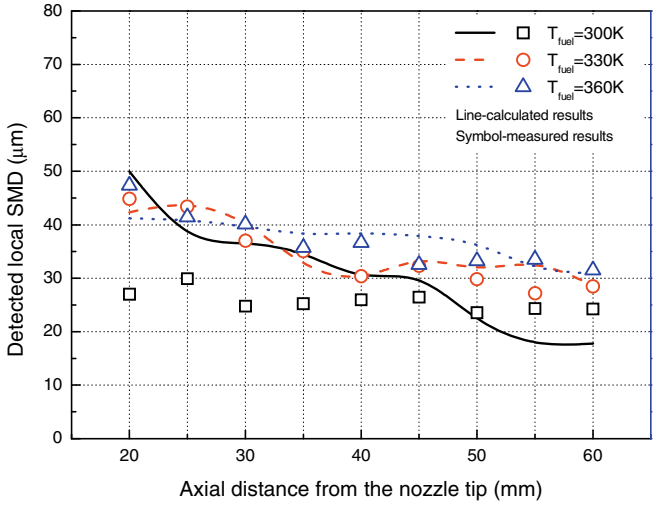

(a) Detected local SMD

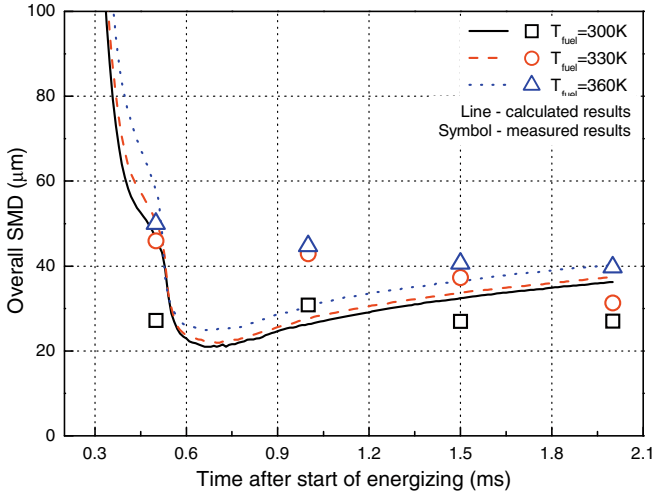

(b) Overall SMD

Fig. 12. Effect of the fuel temperature on the detected local and overall SMD characteristics by experimental and numerical analysis (T_{amb} = 300 K, P_{amb} = 0.1 MPa).

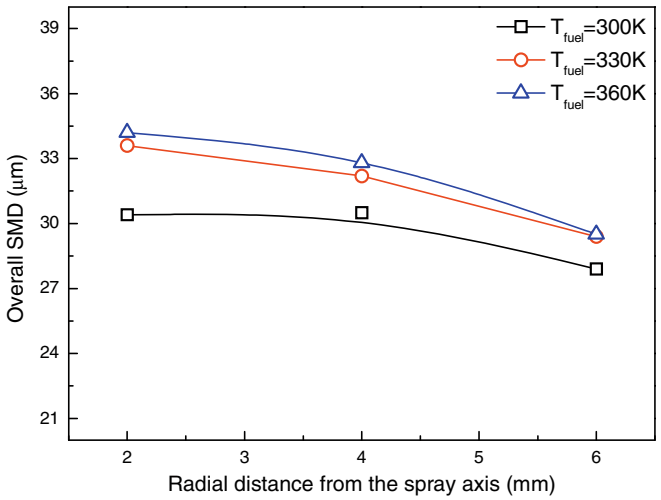

Fig. 13. Overall SMD distributions according to the radial direction.

main. This can be confirmed from the droplet detecting time, which is the time it takes to catch the droplets of the specific numbers. The droplet detecting times for 300 K, 330 K and 360 K fuel temperature are 67 s, 92 s and 113 s, respectively. Droplet detecting time becomes longer with increasing fuel temperatures due to the reduction of the fuel droplet numbers by the evaporation. In addition, the increased fuel temperature induced the high evaporation of the injected fuel droplets, as can be confirmed in Figs. 11 and 14. From these results, it was guessed that these evaporated fuel droplets well mixed with the ambient air. Consequently, this makes the air–fuel mixture to the high quality.

Fig. 12b that represents the overall SMD also shows similar trends as Fig. 12a. The overall SMD also increases with increasing fuel temperature. The overall value is a time dependent droplet size at a specific time in whole measuring points. As shown in Fig. 12b, the measured results decrease a little or become constant, while the calculated results shows the tendency of increase with increasing time after energizing. It can be guessed that the calculated overall SMD was considerably influenced by the droplet coalescence and collision model. In addition, the increasing overall SMD was affected by fuel temperature besides collisions and coalescence of droplets because the evaporation of small droplets after the breakup actively occurred and number of small droplets decreased as the temperature of droplets increased.

Fig. 13 shows the overall SMD distribution according to radial direction. The droplet size of the outer spray became small, and the increased fuel temperature also lead to the increase in the droplet size. Spray droplets in the outer part of the spray had a wide contact area with the ambient air, and had more chances of mixing with the inflow air. These conditions also affect the decrease of droplets diameter at the radial distance.

In this work, the evaporation characteristics of biodiesel fuel were investigated to study the effect of the fuel temperature on the spray-atomization performance, as illustrated in Fig. 14. The evaporation characteristics were analyzed from the number of droplets and the vapor fuel mass by using the numerical method with KIVA-3V. The number of droplets for three test conditions suddenly increased at the early stage of the injection, and then slowly decreased from 1.74 ms (T_{fuel} = 360 K) and 2.21 ms (T_{fuel} = 300 K) after the start of injection. On the other hand, the evaporation rate became large when the fuel temperature increased at the initial injection stage. However, the difference of evaporation rate among three test condition little affect the number of droplets, because the vapor fuel mass is very small. As shown in Fig. 14, the total vapor fuel mass of T_{fuel} = 360 K is always larger than other test conditions, because the initial evaporation rate which was influenced by the fuel temperature is very large. In addition, the vapor fuel mass became uniform from 0.8 ms of the time after the start of energizing. It is the reason why this time is the end of the injection.

Fig. 15 shows the detected droplet percentage of biodiesel fuel at three fuel temperatures. The detected droplet percentage, which means the ratio between the total droplets and the detected droplets in the specific droplet size range, were analyzed at 60 mm from the nozzle tip along the spray axis. As shown in Fig. 15, the ratio of the larger droplet increased and the smaller droplets decreased when the fuel temperature increased, because the increased fuel temperature caused the active droplet evaporation as illustrated in Fig. 14, specially, the small droplets quickly evaporated. These fuel evaporation distribution (Fig. 14) and detected droplet percentage (Fig. 15) supported the detected droplet size distribution which was shown in Fig. 12a.

Fig. 16 shows the mean axial velocity of droplets of biodiesel fuel measured by the droplet measuring system. After the injec-

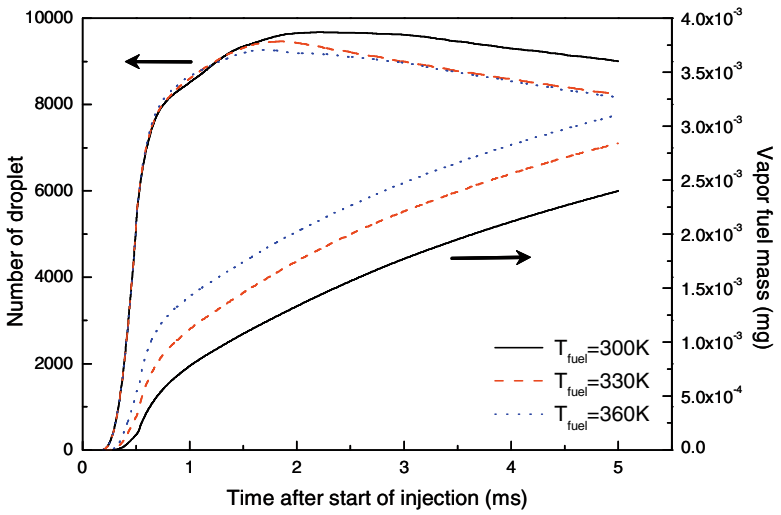

Fig. 14. Calculated evaporation characteristics of biodiesel fuel.

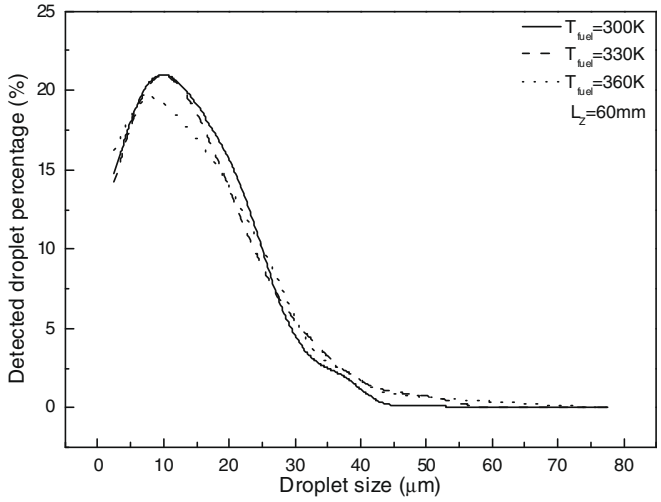

Fig. 15. Droplet detected percentage for the various fuel temperatures (L_Z: axial distance from the nozzle tip).

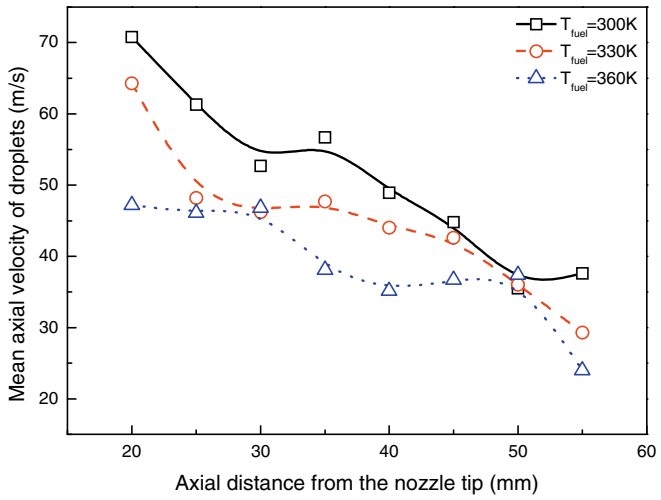

Fig. 16. Maximum axial velocity at different fuel temperature (P_{inj} = 60 MPa, P_{amb} = 0.1 MPa, t_{eng} = 0.5 ms).

tion, the mean axial velocity of droplets decreased along the axial distance from the nozzle tip. This was caused by an increase in the friction and mixing between the injection spray and the ambient air. In addition, the increased fuel temperature results in the decrease of the mean axial velocity of droplets by the reduction of fuel density. The decrease of the fuel density, kinematic viscosity, and surface tension by the increase of the fuel temperature influenced the collision and coalescence between neighbor droplets and the mixing between each droplet and ambient air. Therefore, it can be said that these phenomena result in the decrease of the mean axial velocity of droplets, because the resistance for the movement to the axial direction increased.

5. Conclusions

In this study, spray-atomization behavior of biodiesel fuel derived from soybean oil was investigated at various fuel temperatures and ambient gas conditions. This was done theoretically, through calculated analysis, and experimentally. The conclusions from the experimental and numerical analyses performed in this study are summarized as follows:

1. The spray liquid tip penetration has almost the same patterns regardless of the variation in fuel properties caused by change in the fuel temperature. On the other hand, the increased ambient temperature induced the decrease of the spray liquid tip penetration. Therefore, it can be said that the spray behavior of biodiesel fuel was mainly affected by the ambient air conditions.
2. When the fuel and ambient air temperature increased, the fuel vapor mass also increased. The droplets evaporation occurred most active at the center of the spray. Therefore, it can be expected that the active fuel evaporation by the increase of the fuel and ambient air temperature influences the formation of the homogeneous mixture between the injected fuel spray and ambient air.
3. As the fuel temperature increased, the detected local droplet size at the spray axis also increased, because the small droplets in the detecting volume are more easily evaporated, while the large droplets remain. In the numerical results, the increased fuel temperature induced the active evaporation of injected droplets.
4. Based on the droplet size distribution and evaporation characteristics of injected fuel droplets, SME biodiesel fuel can compose the high quality mixture with ambient air when the fuel temperature and ambient air temperature increases.

Acknowledgements

This work was supported in part by the Center for Environmentally Friendly Vehicle (CEFV) of the Eco-STAR project of the Ministry of the Environment in Seoul, Republic of Korea (MOE). This study was also supported by the Second Brain Korea 21 Project in 2008.

References

Ahmed, M.A., Ejim, C.E., Fleck, B.A., Amirfazli, A., 2006. Effect of biodiesel fuel properties of and its blends on atomization. SAE technical paper, 2006-01-0893.
Amsden, A.A., O'Rourke, P.J., Butler, T.D., 1989. KIVA-II: a computer program for chemically reactive flows with sprays. Los Alamos report, LA-11560-MS, 12-20.
Araneo, L., Soare, V., Payri, R., Shakal, J., 2006. Setting up a PDPA system for measurement in a diesel spray. Journal of Physics: Conference Series 45, 85–93.
Bellman, R., Pennington, R.H., 1954. Effects of surface tension and viscosity on Taylor instability. Quarterly of Applied Mathematics 12, 151–162.
Benedict, R.P., 1980. Fundamental of Pipe Flow, Wiley, New York.
Bianchi, G.M., Falfari, S., Parotto, M., Osbat, G., 2003. Advanced modeling of common rail injector dynamics and comparison with experiments, SAE technical paper, 2003-01-0006.
Desantes, J.M., Payri, R., Salvador, F.J., Gil, A., 2006. Development and validation of a theoretical model for diesel spray penetration. Fuel 85, 910–917.
Faeth, G.M., 1977. Current status of droplet and liquid combustion. Progress in Energy and Combustion Science. 3, 191–224.
Hiroyasu, H., Arai, M., 1990. Structure of fuel sprays in diesel engine. SAE technical paper, 900475.
Kawano, D., Goto, Y., Odaka, M., Senda, J., 2004. Modeling atomization and vaporization processes of flash-boiling spray. SAE technical paper, 2004-01-0534.
Kegl, B., Hribernik, A., 2006. Experimental analysis of injection characteristics using biodiesel fuel. Energy & Fuels 20, 2239–2248.
Kim, M.Y., Bang, S.H., Lee, C.S., 2007. Experimental investigation of spray and combustion characteristics of dimethyl ether in a common-rail diesel engine. Energy & Fuels 21, 793–800.
Lacoste, J., Crua, C., Heikal, M., Kennaird, D., Gold, M., 2003. PDA characterization of dense diesel sprays using a common-rail injection system. SAE technical paper, 2003-01-3085.
Lefebvre, A.H., 1989. Atomization and Sprays. Taylor & Francis.
Ning, W., Reitz, R.D., Diwakar, R., Lippert, A.M., 2008. A numerical investigation of nozzle geometry and injection condition effects on diesel fuel injector flow physics. SAE technical paper, 2008-01-0936.
Nurick, W.H., 1976. Orifice cavitation and its effects on spray mixing. Journal of Fluids Engineering 98, 681–687.

Park, S.H., Yoon, S.H., Suh, H.K., Lee, C.S., 2008. Effect of the temperature variation on properties of biodiesel and biodiesel-ethanol blends fuels. Oil & Gas Science and Technology 63, 737–745.

Ranz, W.E., Marshall, W.R., 1952. Evaporation from drops (parts I and II). Chemical Engineering Progress 48, 141. 173.

Reitz, R.D., 1987. Modeling atomization processes in high-pressure vaporizing sprays. Atomisation and Spray Technology 3, 309–337.

Sarre, C.K., Kong, S.C., Reitz, R.D., 1999. Modeling the effects of injector nozzle geometry on diesel sprays. SAE technical paper, 1999-01-0912.

Suh, H.K., Roh, H.G., Lee, C.S., 2008. Spray and combustion characteristics of biodiesel/diesel blended fuel in a direct injection common-rail diesel engine. Journal of Engineering for Gas Turbine and Power 130 (3). 032817-1∼032807-9.

Yoon, S.H., Park, S.H., Lee, C.S., 2008. Experimental investigation on the fuel properties of biodiesel and its blends at various temperatures. Energy & Fuels 22, 652–656.

Zhu, Y., Reitz, R.D., 2000. Modeling fuel system performance and its effect on spray characteristics. SAE technical paper, 2000-01-1253.